

# Measurements of Spectral Emission and Absorption of a High Pressure Xenon Arc in the Stationary and the Flashed Modes

Lothar Klein

Concurrently with emission measurements of a high pressure xenon arc in the spectral range 3000 Å to 2 μ, its absorption in the ir was measured by a technique based on modulating the less intense radiation of a carbon arc used as background source. The emission measurements were repeated with a rapid scanning spectrometer while flashing the xenon arc for 0.1 sec at 10 kW, which is five times the normal power input. The arc showed excellent stability and reproducibility both in the stationary and the flashed modes. The intensity increase of the continuum was proportional to the increase of power input during the flash. A simple expression was derived connecting the spectral radiance of the continuum directly with the temperature and pressure of the arc. The temperature profile of the xenon arc was obtained using this expression and also by applying the Planck-Kirchhoff method to the Abel inverted emission and absorption of an ir xenon line. Both approaches show fair agreement at the arc center. The wavelength dependence of the correction factor for departures from hydrogenic behavior of the xenon continuum was derived from the measured spectral radiances and compared with theoretical calculations.

## I. Introduction

Emission spectra are extensively used in plasma diagnostics, but only rarely is the absorption of arc plasmas measured quantitatively. One reason seems to be the widely held opinion that arc plasmas at atmospheric pressure viewed over short optical paths are always optically thin, except for the resonance lines. Another reason is the difficulty of finding a suitable background source for absorption measurements. Laboratory plasmas, typically at 10,000°K are so much brighter than the brightest light sources commonly available (e.g., carbon arc or tungsten strip lamp), that the latter are unsuitable. Finally, the methods for deriving the radial distribution of emission and absorption coefficients of optically thick arc plasmas from line-of-sight measurements have been slow to develop, and this has limited the value of absorption spectra for plasma diagnostics. Freeman and Katz were the first to obtain a practical solution for the Abel inversion of plasmas with self-absorption,<sup>1</sup> but a more general approach was only recently found by Elder *et al.*<sup>2</sup> Elder *et al.* also derived the radial temperature profile by the Planck-Kirchhoff method from the Abel inverted emission-absorption measurements. To demonstrate their method, Elder *et al.* used a plasma seeded with sodium and determined the temperature from a sodium resonance line. The peak temperature

was below 3000°K, which is not typical for a laboratory plasma.

Tourin<sup>3</sup> found that the strong ir lines of argon can become optically thick (self-absorbing) at atmospheric pressure. He measured the absorption by a technique based on modulating the radiation from the background source; thus, absorption measurements can be made even when the intensity of the plasma is higher than the intensity of the background source. For the measurements reported in Ref. 3 a tungsten strip lamp could be used, because the mismatch of intensities in the ir is less than at shorter wavelengths. If absorption measurements of plasmas are to be extended into the visible or uv regions of the spectrum, however, a much brighter light source has to be used.

The high pressure xenon arc appears to have the desired characteristics. Since the early measurements of Baum and Dunkelman,<sup>4</sup> its strong continuum in the uv and visible part of the spectrum is known to be considerably more intense than the radiation from the carbon arc. Goncz and Newell's<sup>5</sup> recent work with stationary and flashed xenon arcs covers a more extended spectral range. However, their data were obtained by measuring the spectral irradiance from these arcs and are therefore of limited value for a background source evaluation, where the spectral radiance of the brightest part of the arc is the parameter of interest. The peak temperature of a high pressure xenon arc has been determined by Kopec<sup>6</sup> from wavelength scans of two ir lines, using Bartels' method<sup>7</sup> to estimate the peak temperature of an inhomogeneous plasma from line-of-sight emission measurements of lines showing self-reversal.

The author is with the Warner & Swasey Company, Control Instrument Division, Flushing, New York 11354.

Received 10 October 1967.

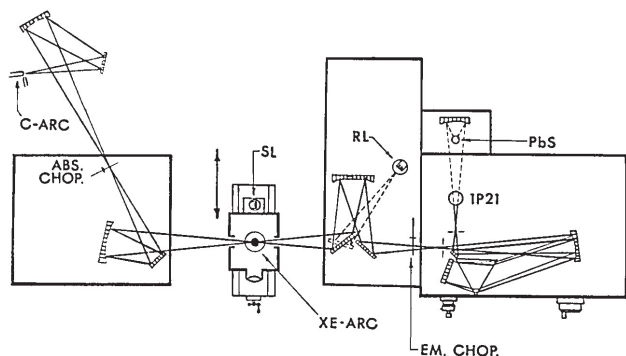


Fig. 1. Optical system used for concurrent measurements of emission and absorption of the stationary xenon arc.

The absorption of a xenon arc has been measured by Rovinskii and Razumtseva,<sup>8</sup> using another xenon arc as a background source. They determined the plasma to be optically thick, but, because of the use of interference filters instead of a monochromator, their measurements were of poor spectral resolution and limited to three wavelength bands in the visible.

It was the primary purpose of the work described here to measure by a refined technique the spectral absorption of the high pressure xenon arc and, simultaneously, its emission. The temperature could then be derived by the Planck-Kirchhoff method. Local values for homogeneous zones of the plasma were obtained by Abel inversion, applying the technique of Elder *et al.*<sup>2</sup> to the absorption measurements. A consistency check was made by comparing the temperature profile of the arc obtained by the Planck-Kirchhoff method with the temperature profile derived independently from the emission measurements of the continuum using the modified Kramers-Unsoeld theory. Since the xenon plasma is optically thick, recourse to seeding as in the work reported in Ref. 2 was unnecessary. Because of its high electron density, the xenon plasma can be expected to be in strict local thermodynamic equilibrium. Thus, these measurements should provide a good case for comparing the emission-absorption method with established diagnostic techniques for plasmas based only on emission.

Concurrently with this program, the spectral radiance measurements were used to evaluate the xenon arc as a background source for absorption measurements of plasmas. We selected a commercially available high pressure xenon arc\* since, as a distinct advantage, this lamp can be flashed at ten times the normal power input for pulse durations of the order of a tenth of a second. The increase of spectral radiance was measured with a rapid scanning spectrometer developed in this laboratory.†

\* Hanovia 491C39.

† Warner & Swasey Model 501 rapid scanning spectrometer.

## II. Experimental

The optical system used for the measurements of the stationary arc is shown schematically in Fig. 1. The xenon lamp housing was mounted on a linear drive table for traversing the arc laterally to the optical axis with a precision of 0.01 mm. Through circular openings in the lamp housing on the two sides along the optical axis, light from the background source could be focused on the xenon arc, and the light emerging from the arc was collected by the foreoptics and focused on the entrance slit of the monochromator. For emission measurements of the arc in the stationary mode, a chopper placed in front of the entrance slit was used; for absorption measurements another chopper modulated only the radiation from the background source. By synchronous rectification of the ac signal from the detector, absorption was measured without interference from the dc signal due to the emission from the xenon arc. This technique of concurrent measurement of emission and absorption has been described in greater detail by Tourin.<sup>9</sup>

The conversion of detector output into units of spectral radiance was achieved by calibration against a tungsten strip lamp, done in two steps. A tungsten strip lamp, held at a constant voltage, was used as a reference lamp and incorporated into the foreoptics of the Perkin-Elmer monochromator (RL in Fig. 1). This type of lamp is also a standard component of the Warner & Swasey Model 501 rapid scanning spectrometer used in conjunction with the flashed xenon arc. The reference lamps can be imaged onto the entrance slit simply by rotating a mirror and their signal compared with the signal for the arc. This is done immediately after each measurement to eliminate errors due to changes in slit setting or electronic drift. From time to time the reference lamp is checked, in turn, against another strip lamp, which is positioned at the same location as the arc and whose spectral radiance is determined, following standard practice, from its

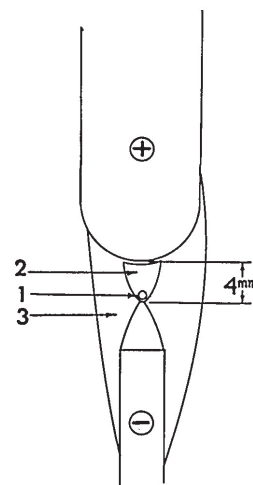


Fig. 2. Zones of different brightness in the high pressure xenon arc: (1) cathode spot, (2) arc plasma, (3) red halo.



temperature accurately measured with an optical pyrometer. It has been our experience that this procedure increases the ease of intensity measurements without loss of accuracy.

The image of the xenon arc projected on a screen appears to the eye as shown in Fig. 2. A small area of intense brightness—the cathode spot—is discernible within the bell-shaped arc plasma. A dim reddish glow partially envelopes the cathode and extends from the cathode to the round tip of the anode. This phenomenon to which no reference in the literature could be found, is called here *red halo*. It has the characteristic of being asymmetric with respect to the arc axis and this asymmetry appeared always at the same location when the arc was started. When the arc is turned off, the red halo does not disappear instantly as does the bright central arc region, but persists over several seconds. We believe that it originates from convectively heated xenon gas streaming upwards from the white hot cathode.

Our measurements were made in a horizontal plane through the arc containing the cathode spot, i.e., the hottest region of the xenon plasma. The entrance slit of both the spectrometers used was masked to a height of 0.25 mm, since spatial scanning of the arc in the vertical direction had shown that near the center, i.e., in the region of major interest, intensity gradients over this length were still small.

In the stationary mode the arc was run at a current of 100 A at 22.5 V. A welder rectifier with line voltage compensator and ripple filter\* proved to be a convenient and stable power supply. By displaying the output of the two detectors (1P21 and PbS) on an oscilloscope, the ac ripple of the light intensity was measured to be less than 2% in both cases. If started from cold, the arc reached a stable regime in about 5 min, then the long term drift measured over 30 min was of the order of 1% for the peak of Xe I 9923 Å, and less than 5% for the continuum at 5000 Å. When the arc was extinguished and restarted with the current control of the rectifier at a fixed position, spatial scanning of the arc proved that the cathode spot always formed at exactly the same location with very good repeatability of light intensity (typically to within 2% for the peak of Xe I 9923 Å).

It is standard practice to use a condenser discharge for flashing the xenon arc<sup>5,6</sup>; the total pulse duration is then at most of the order of a few milliseconds. To make the flashed xenon arc useful as an extremely bright source for absorption measurements in conjunction with modern fast scanning spectrometers, a different approach was followed. A water-cooled stainless steel tube was used as a resistor capable of dissipating a high load and was connected to the rectifier in parallel with the xenon arc. In the *simmering* mode, 100 A flowed through the xenon arc and 450 A through the parallel resistor. A power switch was used to flash the arc by manually opening the

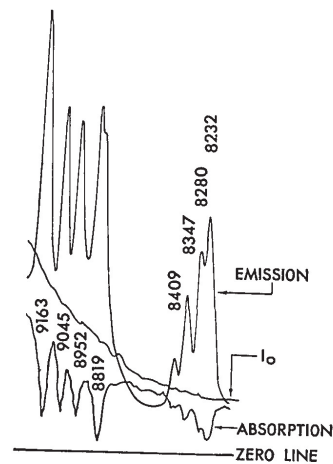


Fig. 3. Strip chart record for emission-absorption measurements of the cathode spot of the xenon arc. The gain was 20 for the emission and 350 for the  $I_0$  and absorption scans. Slit width: 30  $\mu$ .

resistor circuit. Oscilloscope displays showed that after a fast rise time of the order of a few milliseconds, constant lamp current and voltage, i.e., a steady state, was achieved for the duration of the flash (typically 100 msec). For our measurements we flashed the lamp at 10 kW, although double this power is still permissible.

### III. Measurements

#### A. Stationary Mode

A Perkin-Elmer Model 98 monochromator was used and the detector (1P21 tube or PbS) output displayed on a strip chart recorder. Measurements were made in the spectral range from 3000 Å to 2.7  $\mu$ , using a glass prism. Absorption measurements were made with a carbon arc† as background source. We resorted to hand regulation of the arc since the automatic regulator provided by the manufacturer was not sensitive enough for our purpose. The carbon arc operated best under the conditions recommended by Null and Lozier,<sup>10</sup> with a 6.5-mm thick pure graphite anode and the current held at about 11 A just below the hissing point. The use of a 6-mm diam cored cathode (Norris H), however, gave a definite improvement in arc stability over the thin (3.2-mm), pure graphite rod specified by Null and Lozier. This is in agreement with recent observations by Magdeburg and Schley.<sup>11</sup>

Since long term stability of the carbon arc could not be achieved, it proved advisable when measuring the lateral absorption profile, to obtain an  $I_0$  reading in conjunction with every measurement. This was also indicated because of other considerations (see Sec. V. A). Owing to its excellent reproducibility, extinguishing and restarting the xenon arc did not alter its characteristics. A typical emission and absorption record is shown in Fig. 3. The absorptance of Xe I

\* Miller SRH-444-C1 with LVC-8.

† Made by Spindler & Hoyer, Goettingen, W. Germany.

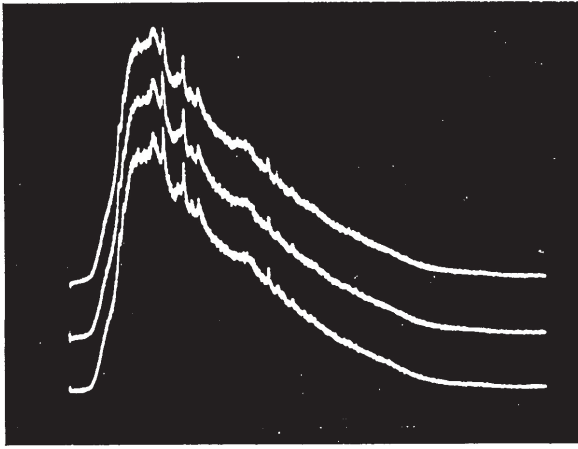


Fig. 4. Oscillogram showing three wavelength scans for a flashed xenon arc. The wavelength range 4200–6500 Å was scanned in 10 msec, using an RCA 4473 photomultiplier. Three flashes are superimposed (total of nine scans shown).

8819 Å, for instance, could be accurately measured to be 91%, although the detector signal for the peak of this line is sixty times stronger than for the carbon arc ( $I_0$  in Fig. 3).

Because of the large number of Xe I lines in the near ir, the wavelength assignment of the lines in the spectrum of the high pressure arc proved to be difficult. Therefore, the following procedure was used: the carbon arc was replaced by a mercury arc and the spectrometer focused at the edge of the xenon arc plasma, where the temperature is lower and consequently the lines are sharper and match better the intensity of the mercury lines. With the emission chopper being used, the xenon and mercury spectra appeared simultaneously; an external wavelength standard had thus become, effectively, an internal standard. The increase in accuracy of wavelength correlation over the standard procedure based on a separately run reference spectrum permitted to assign unambiguously all spectral features of the xenon arc.

## B. Flashed Mode

For the measurements of the flashed xenon arc the Warner & Swasey Model 501 rapid scanning spectrometer was used. This instrument has been described in detail elsewhere.<sup>12</sup> Four detectors (RCA 1P28, 4473, and 7102 photomultipliers, and an InAs photovoltaic detector) were used to scan the xenon spectrum from 3000 Å to 2 μ. Because of the availability of two exit slits, the contiguous spectral ranges for two detectors could be scanned simultaneously.

The scans were displayed on oscilloscopes and recorded photographically. An oscillogram of the flashed xenon arc spectrum in the wavelength range 4200–6500 Å is shown in Fig. 4. For this measurement, the controls of the Model 501 were set for a scanning time of 10 msec, a repetition rate of one scan each 37.5 msec, and a delay of 30 msec. Thus, the start of the first scan occurred 30 msec, of the second 67.5 msec, and of the third scan 105 msec, after the flashing circuit had been

opened. Successive scans are shifted vertically upwards on the oscillogram. To test for reproducibility, the xenon arc was flashed two more times after an interval of a few seconds, and all spectra were recorded on the same photograph. In Fig. 4, each set of three superimposed traces appears as one trace, and all nine traces are identical. Thus, it is proved that the radiation from the xenon arc remains constant during a flash, and that there is excellent flash-to-flash reproducibility. The same results were obtained for two spectral ranges in the near ir from 7000 Å to 1.9 μ. When the experiment was repeated in the uv (3000 Å to 4200 Å) we detected a variation in radiant output during a flash of less than 5%.

Because of the excellent shot-to-shot reproducibility, it was possible to obtain a measure of the plasma absorptance, imaging the cathode spot back on itself by means of a spherical mirror positioned on the optical axis on the opposite side of the xenon arc from the spectrometer. A measurement of emission alone, obtained by placing a shutter in front of the mirror while flashing the arc, was followed by a measurement of emission with added back reflection during a consecutive flash. The reflection and transmission loss of the back-reflected light at the hot quartz envelope, which can be considerable, is difficult to determine. Therefore, measurements of absorption by this technique are inherently inaccurate. It can, however, be determined unequivocally for which lines the absorption is very close to 100%. Thus, the core of Xe I 8232 Å and the self-reversed peak of Xe I 8819 Å in Fig. 5 are black.

## IV. Theory

Following Unsoeld's development of the classical Kramers theory, the emission coefficient (spectral radiance per unit depth) for the combined recombination (*free-bound*) and bremsstrahlung (*free-free*) continuum of an optically thin plasma, expressed in

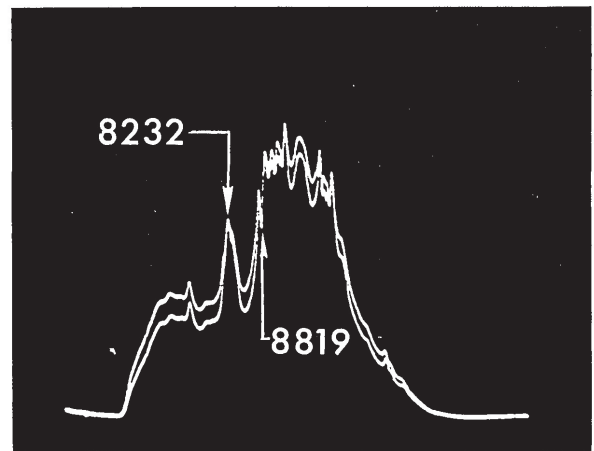


Fig. 5. Wavelength scan of the emission and emission plus back reflection from a mirror of the cathode spot of a flashed xenon arc. The wavelength range 0.7–1.2 μ was scanned in 10 msec using an RCA 7102 photomultiplier.



$W \text{ cm}^{-3}\mu^{-1}\text{sr}^{-1}$ , is given at wavelengths longer than a critical wavelength  $\lambda_c$ , by

$$\epsilon_\lambda = 1.63 \times 10^{-31} [\xi(\lambda)/\lambda^2] (n_e^2/T^{\frac{3}{2}}), \quad (1)$$

with  $\lambda$  in  $\mu$  and  $T$  in  $^\circ\text{K}$ . In deriving Eq. (1), it has been assumed that the ionization stages beyond the first can be disregarded; then the concentration of first ions equals  $n_e$ , the concentration of electrons (condition of plasma quasi-neutrality). The factor  $\xi(\lambda)$  accounts for departures from hydrogenic behavior and quantum mechanical (Gaunt) corrections. Schlueter<sup>13</sup> has calculated  $\xi(\lambda)$  as a function of wavelength at a temperature of 14,000 $^\circ\text{K}$ , although he found this factor to be practically temperature independent.

In the limit of vanishing ionization, Dalton's law and the Saha equation can be combined to a simple expression for the electron density as a function of the state variables  $T$  and  $P$  of the plasma. With the pressure in atm,

$$n_e = 5.953 \times 10^{18} (Q_i/Q_0)^{\frac{1}{2}} P^{\frac{1}{2}} T^{\frac{1}{2}} \exp(-E_i/2kT). \quad (2)$$

For a xenon plasma in the temperature range of 9000–14000 $^\circ\text{K}$ , an average value of 4.44 can be used for  $Q_i/Q_0$ , the ratio of the partition functions for first ions and neutrals, since this value is constant to within 2% in this range, and its pressure dependence is also very small.<sup>14</sup> Substituting  $n_e$  from Eq. (2), with the ionization energy  $E_i = 12.127 \text{ eV}$  (Ref. 14), the emission coefficient for the continuum of a xenon plasma (in  $W\text{cm}^{-3}\mu^{-1}\text{sr}^{-1}$ ) is given, approximately, by:

$$\epsilon_\lambda^{\text{Xe}} = 2.57 \times 10^7 \frac{\xi(\lambda)}{\lambda^2} P \exp(-140,760/T). \quad (3)$$

In order to assess the validity of this expression, we have calculated the electron density for a xenon plasma at 16 atm pressure, using Eq. (2) as compared with the electron density calculated more rigorously using Unsoeld's and also Ecker and Weizel's approach<sup>14</sup> to obtain the lowering of the ionization potential in a plasma. It appears that up to the temperature reached in a high pressure xenon arc (below 12,000 $^\circ\text{K}$ ), the departure of  $n_e$  [Eq. (2)] from  $n_e$  (Unsoeld) is smaller than the discrepancy between  $n_e$  (Unsoeld) and  $n_e$  (Ecker and Weizel). Since there exists no general agreement as to which theoretical approach gives the best quantitative estimate of the lowering of the ionization potential, the inaccuracy in  $n_e$  of less than 20% at the lower temperatures, introduced by the simplifications used in deriving Eq. (2), is of the same order of magnitude as the theoretical uncertainties. Recourse to an elaborate calculation seems therefore hardly to be justified, and, because of its simplicity, Eq. (3) is useful for obtaining the temperature directly from the measured emission coefficient if the pressure is known. The temperature derived by this method is quite insensitive to relatively large errors in the emission coefficient. Thus, it follows from Eq. (3) that an error of 40% results in an error of only 3% in temperature at 11,000 $^\circ\text{K}$ , the peak temperature of the stationary xenon arc, and is still less at lower temperatures.

It follows from Eq. (1) that  $N_\lambda^0$ , the spectral radiance of the continuum measured through the center of an optically thin cylindrical symmetrical xenon plasma of radius  $R$ , is given by

$$N_\lambda^0 = \int_{-R}^R \epsilon_\lambda(r) dr = C \frac{\xi(\lambda)}{\lambda^2} \int_{-R}^R \frac{n_e^2 [P, T(r)]}{T^{\frac{3}{2}}(r)} dr. \quad (4)$$

Unlike the case of line radiation, the integral containing the temperature gradient is not a function of wavelength. Since the  $\xi(\lambda)$  factors are practically temperature independent, relative experimental values for these factors can be obtained directly from line-of-sight measurements of an optically thin plasma. If the temperature profile and the pressure are known, the spectral radiance measurements of the continuum have to be inverted only for one wavelength in order to obtain the  $\xi(\lambda)$  at the other wavelengths without an Abel inversion. The line-of-sight measurements are conveniently related to the emission coefficients at the center of the arc by introducing the equivalent optical pathlength  $L$ :

$$L \equiv [N_\lambda^0 / \epsilon_\lambda(r = 0)]. \quad (5)$$

From an Abel inversion at one wavelength  $\lambda_1$ ,  $\epsilon_{\lambda_1}(r = 0)$  is derived; thus,  $L$  can be calculated and used in turn to derive the emission coefficients at other wavelengths.

The Abel inversion of cylindrically symmetrical plasmas is a straightforward procedure, provided the plasma is optically thin. Different numerical methods are available; we prefer the one proposed by Barr,<sup>15</sup> which combines effective smoothing of small random errors with ease of computation. If the plasma is optically thick, but its minimum measured transmittance higher than about 70–80%, a simple correction procedure suffices. Thus, each intensity measurement has only to be divided by the square root of the transmittance measured along the same line of sight, otherwise the Abel inversion proceeds as in the optically thin case [see Eq. (4) in Ref. 2]. If the transmittance is lower, accurate values of the radial intensity distribution can only be obtained by iteration.<sup>2</sup>

The measurement of plasma absorption is important not only for correcting the emission measurements. If the absorption measurements are also Abel inverted, the radial distribution of emission and absorption can be used to derive the temperature profile of the plasma from first principles (the Planck-Kirchhoff law). In the case of strongly absorbing lines, however, Elder *et al.* in Ref. 2 point out difficulties in performing the Abel inversion of the measured absorption, if monochromators of only moderate wavelength resolution are used. In effect, for large variations of transmittance over the spectral slit width  $\Delta\nu$ , the approximation used,

$$\log \left( \frac{1}{\Delta\nu} \int_{\Delta\nu} \tau(\nu) d\nu \right) \simeq \frac{1}{\Delta\nu} \int_{\Delta\nu} \log \tau(\nu) d\nu, \quad (6)$$

is valid only if the transmittance  $\tau(\nu)$  is larger than about 70% for all frequencies in the internal  $\Delta\nu$ .

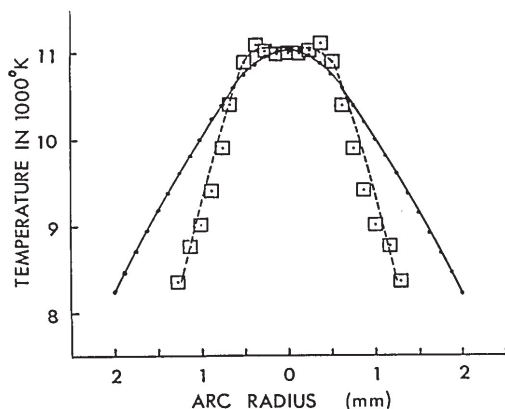


Fig. 6. Radial temperature profile of the cathode spot of the 2.2-kW xenon arc (stationary mode), as obtained from the emission coefficient of the continuum at  $1.31 \mu$  (solid line), and by the Planck-Kirchhoff method from the emission-absorption profile of Xe I 10528 Å (broken line).

## V. Results and Discussion

### A. Radial Temperature Distribution of the Stationary Xenon Arc

The large discrepancy in intensity between the xenon and carbon arc at the shorter wavelengths limited the absorption measurements to the ir region of the spectrum. The accuracy of these measurements is impaired, however, by two effects. When the xenon arc is in operation, its quartz envelope becomes red hot with a marked increase of absorption in the ir. Secondly, the red halo also shows noticeable absorption in the ir and its asymmetry causes an asymmetrical absorption profile. Taking advantage of the persistence of the red halo (see Sec. II), it proved to be advisable to include the absorption of the hot quartz envelope and the red halo in the  $I_0$  reading by recording the signal for the carbon arc radiation at the instant when the xenon arc was extinguished. Even so, the accuracy of the absorption measurements, especially for low absorption near the boundary of the cathode spot, was considerably less than the accuracy of the emission measurements. In the emission measurements, a perfectly symmetrical intensity distribution proved the plasma core to be cylindrical symmetrical. As expected from theory, the curves giving the lateral intensity distribution of the continuum, normalized at peak intensity, were identical at all wavelengths measured.

The Abel inversion requires the measurements to be cut off at a fixed distance from the arc center, where the intensity has gone to zero. Since the region of interest was the hot core of the arc (cathode spot), the boundary of the plasma was drawn somewhat arbitrarily at the point where the intensity had dropped to 1% of its peak value. The intensity of the red halo was of this magnitude and its contribution to the total radiance was thus roughly subtracted. The resulting arc diameter was 4.6 mm. The radial temperature profile was derived by the Planck-Kirchhoff method from the

radial emission and absorption profiles of Xe I 10528 Å, obtained by inverting the lateral emission and absorption measurements of this line. This line was selected because its peak absorption was 28.5% when measured with a spectral slit width which was small compared with the line width; the true peak absorption was therefore still not high enough to lead to difficulties in the inversion of the measured absorption or to make laborious iterations unavoidable. If the absorption is too low, the results become very sensitive to measurement errors. The continuum was therefore not used to derive the temperature profile, but its absorption was measured to correct the emission data for self-absorption. In Fig. 6, the Planck-Kirchhoff temperature profile from the xenon line is compared with the temperature profile derived from the radial emission coefficients of the continuum at  $1.31 \mu$  by application of Eq. (3). The working pressure indicated by the lamp manufacturer (16 atm) and the  $\xi(\lambda)$  value taken from Ref. 13 were substituted in this equation.

As expected, the two temperature profiles agree fairly well near the center of the arc, where the experimental accuracy is higher and diverge toward the periphery. Since the measurement of low intensity is inherently more accurate than the measurement of low absorption, more credence is given in this region to the temperature profile derived from the corrected continuum intensity. It is noteworthy that the temperature gradient appears to have a constant value (1600°K/mm) from close to the arc center to the periphery.

From the inverted emission coefficient  $\epsilon(\lambda = 1.31 \mu, r = 0)$ , the equivalent optical path length as defined by Eq. (5) is calculated to be  $L = 0.14$  cm. To a good approximation, the spatially averaged spectral radiance  $N_\lambda^0$  of the continuum at other wavelengths obtained by line-of-sight measurements through the arc center is therefore equivalent to the emission coefficient of a homogeneous xenon plasma of 0.14-cm diam at 11,050°K and 16 atm. Using Eq. (3), the correction factors  $\xi(\lambda)$  can then be related directly to the measured spectral radiance  $N_\lambda^0$ :

$$N_\lambda^0 = 178[\xi(\lambda)/\lambda^2]. \quad (7)$$

The  $\xi(\lambda)$  values derived from our measurements of the stationary xenon arc are plotted on Fig. 7 and compared with correction factors calculated from theory by

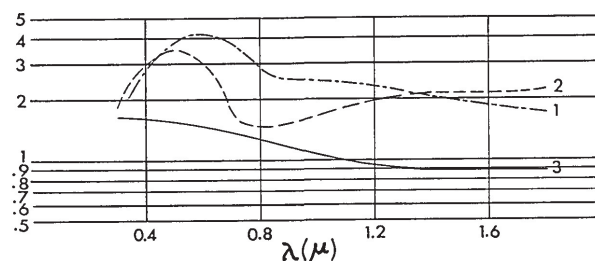


Fig. 7. Experimental  $\xi(\lambda)$  factors for the xenon continuum compared with calculated values: (1) This paper, (2) Schlueter,<sup>13</sup> (3) Biberman *et al.*<sup>16</sup>



**Table I. Emission and Absorption Measurements and Average Temperature (Planck-Kirchhoff) of the Cathode Spot of the Xenon Arc in the Stationary Mode**

	$\lambda(\text{\AA})$	$N_{\lambda 0}$ ( $\text{W cm}^{-2}$ $\text{sr}^{-1} \mu^{-1}$ )	Absorp- tion (%)	$\bar{T}$ ( $^{\circ}\text{K}$ )
Xe I	8232	5,900	89	10,020
cont	8500	1,615	23	10,750
Xe I	8819 (peak)	4,390	97	9,160
	(wing)	4,960	90	10,500
Xe I	9800	3,400	89	9,820
Xe I	9923	3,340	90	9,840
Xe I	10528	892	28.5	9,950
Xe I	11742	906	42.5	9,400
Xe I	12623	640	37	9,920
cont	13100	213	17	8,870
Xe I	14733	575	55	10,060
Xe I	15418	317	37	9,840

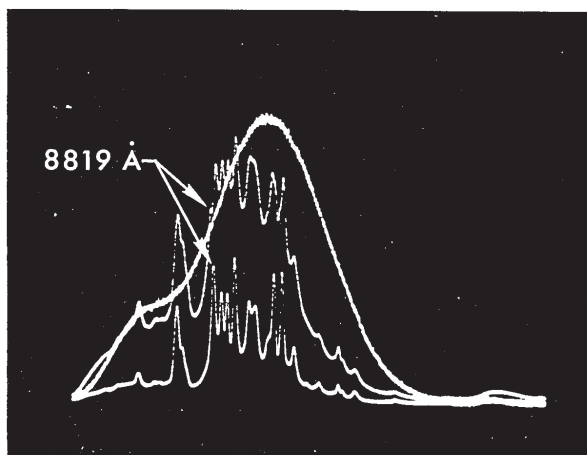


Fig. 8. Wavelength scan in the range 0.7–1.2  $\mu$  for the stationary (lower trace) and flashed xenon arc (both at same gain and with 0.1-mm slit widths) and the reference tungsten strip lamp (1-mm slit widths).

Biberman *et al.*<sup>16</sup> and by Schlueter,<sup>13</sup> as taken from Fig. 4 of Ref. 13. It can be seen that the general shape of Schlueter's curve is borne out by our experimental values, although the peak in the visible appears shifted toward the red. While the relative values of the experimental  $\xi(\lambda)$  appear well established, this is not true for the absolute values in view of the uncertainties in the plasma pressure, which could not be measured. Since we substituted Schlueter's value for  $\xi(1.31 \mu)$  in Eq. (3), the curve of the experimental correction factors has been obtained essentially by normalizing for the  $\xi(1.31 \mu)$  value given by Schlueter.

### B. Line-of-Sight Measurements of the Xenon Arc

In Table I, the emission-absorption data for representative ir lines and continua are presented, corresponding to line-of-sight measurements through the center of the stationary xenon arc.

The tabulated temperatures have been derived by the Planck-Kirchhoff method from the measured peak emission and absorption and are not dependent on the slit function of the spectrometer.<sup>17</sup> Although the tabulated temperatures are only average temperatures, because of the temperature gradient along the line of sight, these average temperatures are weighted strongly toward the center of the arc and are only about 10% lower than the peak temperature. Since all measured lines originate from closely spaced high lying states, an influence of the upper energy level on the average temperature is not apparent. It is shown, evident, however, that strongly absorbing lines give a lower temperature. This effect is shown clearly for Xe I 8819  $\text{\AA}$ , whose self-reversed center is almost black and gives a lower temperature than the false peak in the wing. The self-reversal of this line increases markedly at the higher temperatures of the flashed arc as shown on Fig. 8. While only Xe I 8819  $\text{\AA}$  appears self-reversed in our spectra of the stationary and flashed arc, four lines become black in the center when the arc is flashed. The peaks of these lines lie on the blackbody curve for 11,300 $^{\circ}\text{K}$  as shown on Fig. 9 where the spectral radiance of the stationary and flashed xenon arc has been plotted against wavelength. From the measured radiance and this temperature (11,300 $^{\circ}\text{K}$ ), a value for the absorption was calculated for the other lines and these values are consistent with the reflection data. It appears, therefore, that also for the flashed xenon arc all ir lines give essentially the same average Planck-Kirchhoff temperature.

The temperature increase during the flash is borne out by the strong enhancement of the only ion line in the scanned spectrum (Xe II 5292  $\text{\AA}$ ). In contrast, the strong, self-absorbed atomic lines in the ir have only double the intensity of the same lines in the stationary arc. The intensity increase of the continuum is around 4–4.5 times, matching closely the increase of electrical power input.

It appears plausible for rough estimates to attribute the intensity increase of the continuum to an increase of temperature alone, since the increase of pressure and optical pathlength during the flash is expected to be much less significant. It follows then from Eq. (3) that a 4.5-fold increase of spectral radiance of the continuum of a xenon plasma originally at 9950 $^{\circ}\text{K}$  (the average Planck-Kirchhoff temperature of the stationary arc) corresponds to an increase of the temperature to 11,150 $^{\circ}\text{K}$ , very close to 11,300 $^{\circ}\text{K}$ , the average Planck-Kirchhoff temperature of the flashed arc.

Our measurements can be compared with Kopec's<sup>6</sup> work; he studied the emission from the cathode spot of a similar xenon arc\* in the wavelength range 8200–9000  $\text{\AA}$ . His values for the spectral radiance of the two strongest xenon lines show fair agreement with our measurements. Thus he measured 5800  $\text{W cm}^{-2} \text{sr}^{-1} \mu^{-1}$  and 4100  $\text{W cm}^{-2} \text{sr}^{-1} \mu^{-1}$  for the peak of Xe I 8232  $\text{\AA}$  and for one of the false peaks of the self-reversed

\* Osram XBO 500.

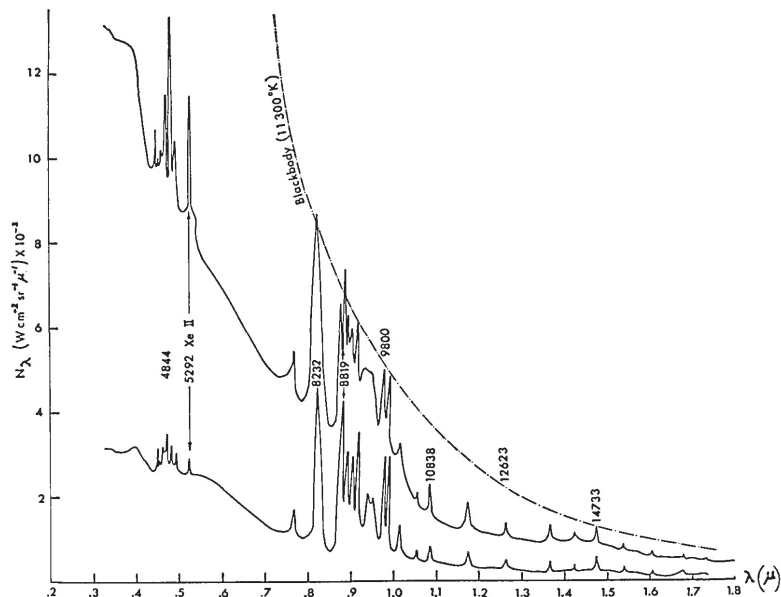


Fig. 9. Measured spectral radiance of the cathode spot of the high pressure xenon arc: in the stationary mode at 2.2 kW power (lower trace), and flashed for 0.1 sec at 10 kW (upper trace).

line Xe I 8819 Å (see Fig. 6 of Ref. 6\*), respectively, while our equivalent values are  $5900 \text{ W cm}^{-2} \text{ sr}^{-1} \mu^{-1}$  and  $4960 \text{ W cm}^{-2} \text{ sr}^{-1} \mu^{-1}$  (see Table I). Kopec used the false peak of this self-reversed line to determine the temperature of the center of the cathode spot from a line-of-sight measurement. He takes as the lower bound the brightness temperature derived from the measured spectral radiance ( $8700^\circ\text{K}$ ) and as the upper bound the temperature given by Bartels<sup>7</sup> theory ( $10,300^\circ\text{K}$ ). As the true peak temperature of the cathode spot he uses the arithmetic mean of these two temperatures, obtaining  $9500^\circ\text{K}$ . This appears to be low and in view of the agreement in measured spectral radiance between Kopec's and our work, this temperature is difficult to reconcile with our value of  $11,000^\circ\text{K}$ , obtained more rigorously by an Abel inversion.

## VI. Conclusions

Because of its very intense, smooth continuum in the near uv and visible spectral region, the high pressure xenon arc appears promising as a useful background source for absorption measurements of plasmas. It has been shown that by a flashing technique the continuum intensity of the xenon arc can still be increased by perhaps as much as an order of magnitude for durations of about 0.1 sec, and, if adequate power supplies are used, the excellent stability and reproducibility of the stationary xenon arc are conserved. Employing modern fast scanning spectrometers, measurements can be made during these long flashes without loss of spectral range or resolution.

A comparison of the temperature profile of the xenon arc with the Planck-Kirchhoff temperature obtained

from a line-of-sight measurement of emission and absorption of ir xenon lines, shows that these average temperatures are weighted strongly toward the peak temperature and are meaningful parameters (as opposed to brightness temperatures obtained from emission measurements alone) and can be useful for the evaluation of high pressure arcs of the noble gases. It appears, however, that the presence of large asymmetric boundary layers makes it difficult to determine the absorption profiles of free burning arcs of the type investigated. Confined arcs, e.g., the wall-stabilized arc, may be better indicated as light sources for accurate work involving the concurrent measurement of plasma emission and absorption.

The author wishes to thank H. J. Babrov for many helpful discussions and comments and A. Healy for assistance in the measurements and calculations. This research was partially supported by NASA.

## References

1. M. P. Freeman and S. Katz, *J. Opt. Soc. Amer.* **50**, 826 (1960).
2. P. Elder, T. Jerrick, and J. W. Birkeland, *Appl. Opt.* **4**, 589 (1965).
3. R. H. Tourin, *J. Quantum Spectrosc. Radiat. Transfer* **3**, 89 (1963).
4. W. A. Baum and L. Dunkelman, *J. Opt. Soc. Amer.* **40**, 782 (1950).
5. J. H. Gonce and P. B. Newell, *J. Opt. Soc. Amer.* **56**, 87 (1966).
6. U. Kopec, *Ann. Phys.* **7/12**, 209 (1963).
7. H. Bartels, *Z. Phys.* **128**, 546 (1950).
8. R. E. Rovinskii and G. P. Razumtseva, *Opt. Spectrosc.* **7**, 431 (1959).
9. R. H. Tourin, *Temperature, Its Measurement and Control in Science and Industry*, C. M. Herzfeld, Ed. (Reinhold Publishing Co., New York, 1962), Vol. III, p. 459.

\* The units used for the ordinate in this figure are incorrect.



10. M. R. Null and W. W. Lozier, *J. Opt. Soc. Amer.* **52**, 1156 (1962).  
 11. H. Magdeburg and U. Schley, *Z. Angew. Phys.* **20**, 465 (1966).  
 12. S. A. Dolin, H. A. Kruegle, and G. J. Penzias, *Appl. Opt.* **6**, 267 (1967).  
 13. D. Schlueter, *Z. Astrophys.* **61**, 67 (1965).

14. H. W. Drawin and P. Felenbok, *Data for Plasmas in Local Thermodynamic Equilibrium* (Gauthier-Villars, Paris, 1965).  
 15. W. L. Barr, *J. Opt. Soc. Amer.* **52**, 885 (1962).  
 16. L. M. Biberman, G. E. Norman, and K. N. Ulyanov, *Opt. Spectrosc.* **10**, 297 (1961).  
 17. H. J. Babrov, *J. Opt. Soc. Amer.* **51**, 171 (1961).

Transmission Fringes in Reflection Multiple-Beam Interferometry	Jose Pastor and Paul H. Lee	149
Interferometric Method for Measuring the Thermal Expansion of Small Samples of Optical Materials	Stanley S. Ballard, James Steve Browder, Hoyt M. Kaylor, and John L. Streete	155
Coma Correction in Czerny-Turner Spectrographs	Charly D. Allemand	159
Optical Properties of Some Transition Metals	D. W. Juenker, L. J. LeBlanc, and C. R. Martin	164
Cauchy Analysis of Imaginary-Dielectric-Index Bands	G. Andermann and L. R. Brantley	171
Classical Coherence Formulation Formulation of Second-Harmonic Generation in the Optical Parametric Amplifier	Joel L. Zuckerman and John B. DeVelis	175
Strengths of Forty-two Lines in the $\nu_1$ and $\nu_3$ Bands of Water Vapor	Harold J. Babrov and Frank Casden	179
Low-Resolution Determination of the Strength of the $667\text{-cm}^{-1}$ $\text{CO}_2$ Band	C. N. Harward and R. R. Patty	188
Net Internal for Calculating Absorption Spectra	Thomas G. Kyle	192
Afterglow Spectrum of a rf Mercury Discharge	James A. Aubrecht, Bruce M. Whitcomb, Richard A. Anderson, and Robert C. Pickett	196
Continuum Radiation Source of High Intensity	P. Bogen, H. Conrads, G. Gatti, and W. Kohlhaas	203
Optical Faraday Effect in Atomic Hydrogen	Jack Finkel	207
Experimental Study of Optical Second-Harmonic Generation in Silver	H. Sonnenberg and H. Heffner	209
Electric-Field and Multiple-Foil Excitation Experiments on Beam-Foil-Excited Hydrogen Atoms	William S. Bickel	213
Measurement of Extinction Coefficients of Triplet Absorption and Quantum Yields of Triplet Formation	William R. Dawson	222
Bandwidth Dependence of Measured uv Absorption Cross Sections of Argon	Robert D. Hudson and Virginia L. Carter	227
Triplet-Triplet Absorption Spectrum (4500-3800 Å) of Perdeuteronaphthalene in Polymethylmethacrylate under Very High Pressures	Malcolm Nicol and John Somekh	233
Binding Energies of Electrons in the Next Inner Subshell of Atoms and Ions from Boron to Zinc	Wolfgang Lotz	236
Information Reduction in Holograms for Visual Display	C. B. Burckhardt	241
Conversion of Millimeter-Wave Images Into Visible Displays	H. Jacobs, R. Hofer, G. Morris, and E. Horn	246
Visual Disinhibition with Binocular and Interocular Presentations	Daniel N. Robinson	254
Luminance Requirements for Hue Perception in Small Targets	Mary M. Connors	258
Increment-Threshold Spectral Sensitivity of the Rhesus Monkey as a Function of the Spectral Composition of the Background Field	H. G. Sperling, N. A. Sidley, W. S. Dockens, and C. L. Jolliffe	263
Letters to the Editor:		

Refractive Indices of Liquid Crystal Cholestery 2-(2-Ethoxyethoxy) Ethyl Carbonate	L. Kopf	269
Decay of Metastable Helium Molecules ( $^3\Sigma_u^+$ ) and Atoms ( $^3S$ ) in an Afterglow	Kenneth H. Ludlum, James M. Caffrey, Jr., and Lewis P. Larson	269
Extinction Coefficient of Bentonite Determined from the Opacity of Bentonite-Water Suspensions	H. D. Weymann and M. G. Chaung	271
Light Scattering in Paper and Its Effect on Halftone Reproduction	Hiromu Wakeshima, Tatsuo Kunishi, and Shohei Kaneko	272
Holographic Imaging Through a Random Medium	H. Kogelnik and K. S. Pennington	273
Note on the Fast Fourier Transform	A. K. Rigler	274
Calculated $\nu$ Values of the Levels of the $5p^4$ Configuration of Te I	G. W. Charles	275
Holographic Imaging Through Scatters	H. J. Caulfield	276
Proposed Reference Index for Typical American Glasses	P. Rajagopala Rao, R. N. Chatterjee, and D. V. Singh	277
Optical Constants of Sodium Chloride and Potassium Chloride in the Far Ultraviolet	D. M. Roessler and W. C. Walker	279
Total Scattering and Absorption by Spheres where $m \approx 1$	Douglas M. Moore, F. Dudley Bryant, and Paul Latimer	281
Measurement of Optical Surface-Wave Attenuations on Plane Liquid-Air Interfaces	R. H. Dungan and H. C. Bryant	283

Book Reviews

Laser Systems and Applications, By Herbert A. Eliot	Reviewed by Edward V. Ashburn	284
Revision of NBS Tables of Spectral-Line Intensities Below 2450 Å. By Charles Corliss		284
Optical Rotatory Dispersion and Circular Dichroism in Organic Chemistry, Edited by G. Snatzke	Reviewed by Wallace R. Brode	285
Geometrische Optik, By H. G. Zimmer	Reviewed by L. Ivan Epstein	285
Techniques of Vacuum Ultraviolet Spectroscopy, By James A. R. Samson	Reviewed by J. C. Boyce	285
Fiber Optics: Principles and Applications, By N. S. Kapany	Reviewed by Alan L. Jones	286
Photoionization Processes in Gases, By Geoffrey V. Marr	Reviewed by James A. R. Samson	287
High Energy Beam Optics, By Klaus G. Steffen	Reviewed by T. Yamanouchi and A. C. Melissinos	287
Handbook of Fluorescence Spectra of Aromatic Molecules, By Isadore B. Berlman	Reviewed by Ferd Williams	287
Theory of Spectrochemical Excitation, By P. W. J. M. Boumans	Reviewed by Charles H. Corliss	287
Spectroscopy, Volume Two: Ultraviolet, Visible, Infrared and Raman Spectroscopy, By S. Walker and H. Straw		288
Optical Interferometry, By M. Françon	Reviewed by Shirleigh Silverman	288
Handbuch der Lichttechnischen Literatur	Reviewed by F. M. Phelps III	288
	Edited by Joachim Riege and Alfred Kurrek	289

Announcement

Contents	289
Optik, Band 25, Heft 6; Optik, Band 26, Heft 1	289
Technical Groups	289
Technical Notes	290
Carl C. Kiess	292
Matthew Luckiesh	293
Technical Calendar	293
Local Section Calendar	293
Annual Report of Treasurer, Optical Society of America, Inc.	294
From the Executive Office	295
Editor's Page	296